

Hysteretic behavior studies of self-centering energy dissipation bracing system

Longhe Xu ^{*1}, Xiaowei Fan ¹, Dengcheng Lu ¹ and Zhongxian Li ²

¹ School of Civil Engineering, Beijing Jiaotong University, Beijing 100044, China

² Key Laboratory of Coast Civil Structure Safety of China Ministry of Education, Tianjin University, Tianjin 300072, China

(Received October 27, 2015, Revised January 22, 2016, Accepted February 11, 2016)

Abstract. This paper presents a new type of pre-pressed spring self-centering energy dissipation (PS-SCED) bracing system that combines friction mechanisms between the inner and outer tube members to provide the energy dissipation with the pre-pressed combination disc springs installed on both ends of the brace to provide the self-centering capability. The mechanics and the equations governing the design and hysteretic responses of the bracing system are outlined, and a series of validation tests of components comprising the self-centering mechanism of combination disc springs, the friction energy dissipation mechanism, and a large scale PS-SCED bracing specimen were conducted due to the low cyclic reversed loadings. Experimental results demonstrate that the proposed bracing system performs as predicted by the equations governing its mechanical behaviors, which exhibits a stable and repeatable flag-shaped hysteretic response with excellent self-centering capability and appreciable energy dissipation, and large ultimate bearing and deformation capacities. Results also show that almost no residual deformation occurs when the friction force is less than the initial pre-pressed force of disc springs.

Keywords: self-centering energy dissipation brace; combination disc spring; hysteretic behavior; residual deformation; low cyclic reversed loading test

1. Introduction

Conventional earthquake-resistant structural systems, such as moment-resisting frames, shear wall structures or concentrically braced systems, are expected to provide adequate safety and experience large inelastic deformations for design level earthquakes, which will inevitably cause the structural damage and the occurrence of residual deformations. Because of the structural damage and residual deformations, some buildings are difficult to repair and have to be demolished and rebuilt, which results in huge economic losses and also affects the normal use. It is advantageous to develop the self-centering system with the ability of energy dissipation to reduce the structural damage and the self-centering ability to return to the initial position of the system after an earthquake, such as those systems exhibiting flag-shaped hysteretic responses. The moment-resisting frames with steel post-tensioned self-centering connections and supplemental energy dissipation devices had been experimentally and analytically developed by several

*Corresponding author, Professor, E-mail: lhxu@bjtu.edu.cn

researchers (Garlock *et al.* 2005, 2007, Morgen and Kurama 2007, 2008, Kim and Christopoulos 2009, Xu *et al.* 2014, Zhou *et al.* 2014, Cao *et al.* 2015), and these connections were able to undergo large deformations with good energy dissipation and self-centering capabilities.

Conventional braces designed according to the latest earthquake-resistant design standards are deemed to provide adequate seismic safety for structures during earthquakes, buckling restrained braces (BRBs), which are able to yield in both tension and compression, have been developed to overcome the buckling of conventional braces (Sabelli *et al.* 2003, Uang *et al.* 2004), however, large residual deformations may exist in BRBs and structures after moderate earthquake and costly repairs might be necessary (Marino and Nakashima 2006, Zhu and Zhang 2007). To address these drawbacks, some self-centering braces with flag-shaped hysteretic performance were developed (Miller 2011, Miller *et al.* 2011, 2012), which utilized the superelastic shape memory alloy rods or pre-stressed steel strands to provide the self-centering capability to reduce or eliminate the residual deformations. Christopoulos *et al.* (2008) proposed a self-centering energy dissipation brace which used friction devices to dissipate energy, and a set of fiber-reinforced polymer tensioning elements to provide self-centering capacity. A reusable hysteretic damping brace with the energy dissipation component made up of superelastic Nitinol wires or friction devices was developed by Zhu (Zhu and Zhang 2007, 2008), which exhibited self-centering hysteretic responses and outstanding fatigue properties. Seismic analyses of braced frames have confirmed that the structures with self-centering energy dissipation braces have smaller residual deformations than those systems with BRBs after earthquakes (Tremblay *et al.* 2008, Erochko and Christopoulos 2014).

In this paper, a new type of pre-pressed spring self-centering energy dissipation (PS-SCED) bracing system that combined friction mechanisms between the inner and outer tube members to provide the energy dissipation with the pre-pressed combination disc springs installed on both ends of the brace to provide the self-centering ability was developed. The configuration and mechanical behaviors of PS-SCED bracing system were described, and experiments of the self-centering mechanism of disc springs, the friction energy dissipation mechanism, and a large scale PS-SCED bracing specimen were conducted due to the low cyclic reversed loadings to demonstrate the behaviors of the bracing system.

2. Mechanics of PS-SCED brace

The PS-SCED bracing system consists of two tube members, the outer tube and inner tube, which can slide past each other, the pre-pressed disc springs that provide the self-centering force, and friction energy dissipation mechanisms (FEDMs), as shown in Fig. 1. Four pieces of steel plates are welded to the inner tube to improve the bearing and deformation capabilities of the PS-SCED bracing system, and several blocking plates are welded to the two tube members to extrude the combination disc springs to increase the self-centering ability. The FEDMs are connected to the two tube members and are activated when the relative motion occurs between the two members. The initial pre-pressed force of combination disc springs and friction force of FEDMs provide the bearing force of the bracing system for normal service condition. Once the relative motion between the two tubes occurs, the friction force of the FEDMs changes from static friction force to kinetic friction force, to dissipate the input energy, the pre-pressed disc springs' compression deformation increases regardless the brace is in compression or in tension. If the initial force of pre-pressed disc springs can overcome the force desired to activate the FEDMs, a full self-centering behavior can be achieved to reduce or eliminate the residual deformations.

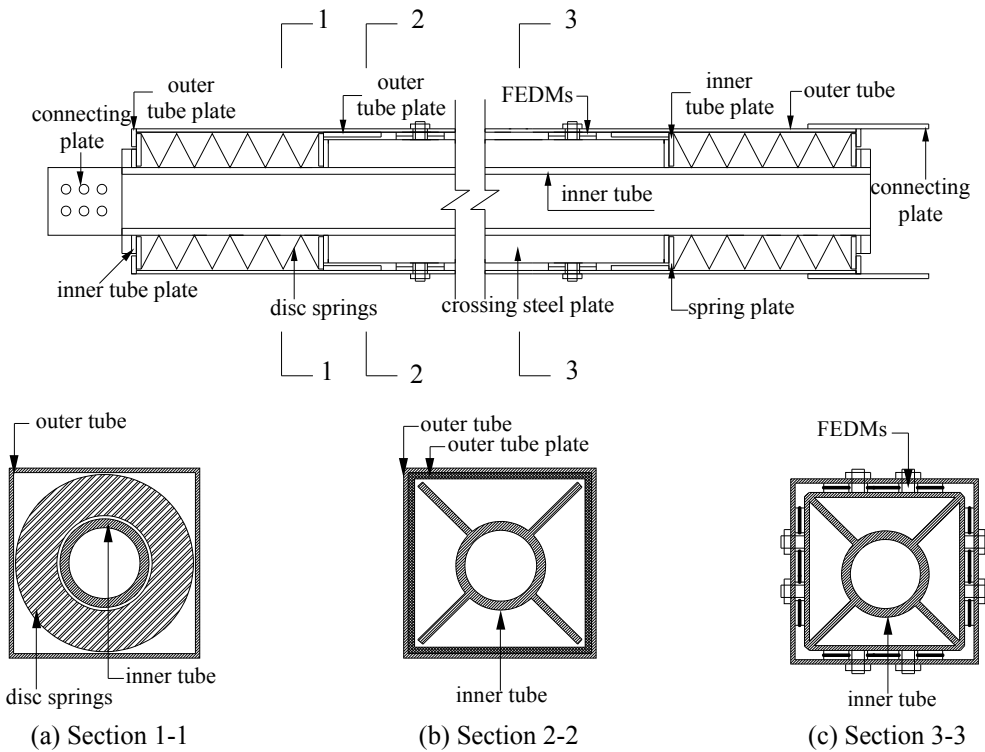


Fig. 1 Configuration of PS-SCED brace

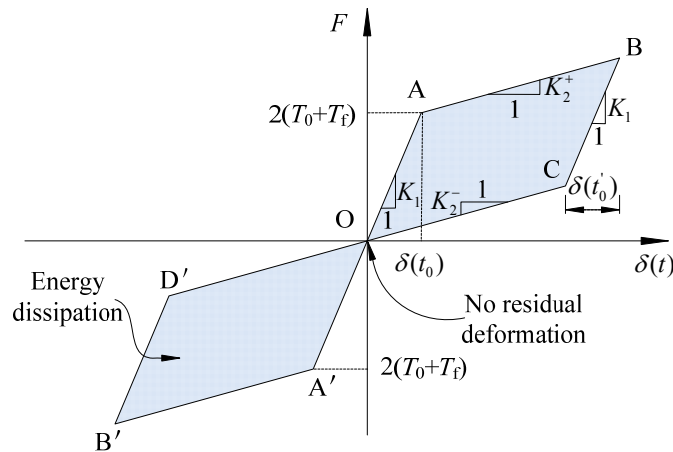


Fig. 2 Flag-shaped hysteretic behavior of PS-SCED brace

The PS-SCED bracing system is expected to exhibit a repeatable flag-shaped hysteretic response with full self-centering capability, Fig. 2 shows the hysteretic response of PS-SCED brace under one circle of horizontal low cyclic reversed loading, and the mechanical response can be divided into different stages in tension or compression according to the changes of stiffness. The PS-SCED bracing system in tension experiences four stages, OA stage as shown in Fig. 2, the

relative motion between the two tube members doesn't occur, the inner or outer tubes stiffness is considerably larger than the stiffness of one side of disc springs, and the deformation of brace is mainly determined by that of the two tube members, thus the stiffness of the whole brace, K_1 , is given by

$$K_1 = \frac{K_i \cdot K_o}{K_i + K_o} \quad (1)$$

where K_i and K_o are the axial stiffness of the inner tube and outer tube, respectively.

AB stage, the relative motion between the two tube members starts to the target deformation, the stiffness of the brace, K_2^+ , is mainly controlled by the combination disc springs, which is approximately equal to the stiffness of springs

$$K_2^+ = 2U_f^+ K_s \quad (2)$$

$$U_f^+ = \frac{1}{1 - U_M(n-1) - U_R} \quad (3)$$

where K_s is the stiffness of one side of combination disc springs, U_f^+ is the friction coefficient of disc springs when the PS-SCED brace is loaded, n is the number of the same specification disc springs at the same direction, U_M is the friction coefficient of disc spring cone, and U_R is the friction coefficient at the bearing edge of disc springs.

BC stage, the bracing system begins to unload, and the relative motion between the two tube members doesn't occur because of the friction of combination disc springs and FEDMs, which is similar to the first stage, OA stage, the stiffness of the brace, K_1 , is mainly controlled by the two tube members.

CO stage, the bracing system is in the self-centering stage which is similar to the second stage of loading, AB stage, and the stiffness of the whole brace, K_2^- , is given by

$$K_2^- = 2U_f^- K_s \quad (4)$$

$$U_f^- = \frac{1}{1 + U_M(n-1) + U_R} \quad (5)$$

where U_f^- is the friction coefficient of disc springs when the PS-SCED brace is unloaded.

The PS-SCED bracing system in compression also experiences four stages, OA', A'B', B'C', C'O stage, as shown in Fig. 2, the mechanical behaviors are similar to that of the bracing system in tension. For the proposed PS-SCED bracing system to function, the two tube members must be capable of bearing significant axial forces without failure or yielding and the combination disc springs should have enough stiffness to produce the restoring force that is required to assure the self-centering capacity of the system.

According to the elastic deformation of the inner and outer tubes, the bilinear elastic model of combination disc springs and the ideal elastic-plastic model of friction devices, the restoring force of PS-SCED brace in tension can be obtained as follows

$$F = \begin{cases} K_1 \delta(t) & 0 < \delta(t) < \delta(t_0) \text{ and } \delta(t) \cdot \dot{\delta}(t) > 0 \\ K_1 \delta(t_0) + K_2^+ (\delta(t) - \delta(t_0)) & \delta(t_0) < \delta(t) < \delta(t_{\max}) \text{ and } \delta(t) \cdot \dot{\delta}(t) > 0 \\ K_1 (\delta(t_0) + \delta(t) - \delta(t_{\max})) + K_2^+ (\delta(t_{\max}) - \delta(t_0)) & \delta(t_{\max}) - \delta(t'_0) < \delta(t) < \delta(t_{\max}) \text{ and } \delta(t) \cdot \dot{\delta}(t) < 0 \\ K_1 (\delta(t_0) - \delta(t'_0)) + K_2^+ (\delta(t_{\max}) - \delta(t_0)) - K_2^- (\delta(t_{\max}) - \delta(t'_0) - \delta(t)) & 0 < \delta(t) < \delta(t_{\max}) - \delta(t'_0) \text{ and } \delta(t) \cdot \dot{\delta}(t) < 0 \end{cases} \quad (6)$$

where

$$\delta(t_0) = \frac{2(T_0 + T_f)}{K_1} \quad (7)$$

$$\delta(t'_0) = \frac{T_0 (U_f^+ - U_f^-) + K_2^+ (\delta(t_{\max}) - \delta(t_0)) - K_2^- (\delta(t_{\max}) - \delta(t_0)) + 4T_f}{K_1} \quad (8)$$

where T_0 is the initial pre-pressed force of one side of disc springs, T_f is the friction force provided by one side of friction devices, $\delta(t)$ is the deformation of the PS-SCED brace in compression or in tension, $\delta(t_0)$ is the maximum deformation of brace before the relative motion between the two tube members occur when the bracing system is loaded, and $\delta(t'_0)$ is the maximum relative deformation of brace before the relative motion between the two tube members occur when the bracing system is unloaded, $\delta(t_{\max})$ is the maximum target deformation of brace.

When the residual deformation, δ_r , occurs, it is given by

$$\delta_r = \frac{K_1 (\delta(t'_0) - \delta(t_0)) - K_2^+ (\delta(t_{\max}) - \delta(t_0))}{K_2^-} + \delta(t_{\max}) - \delta(t'_0) \quad (9)$$

3. Hysteretic behavior tests of PS-SCED bracing system

3.1 Validation of combination disc springs

For the proposed PS-SCED brace to function, the combination disc springs must be capable of undergoing significant axial compression deformation without failure or yielding in order to assure the self-centering capacity of the system. The stiffness, deformation and bearing force can be easily obtained through theoretical analysis, in order to validate the self-centering behavior of disc springs, the experiments were conducted on two kinds of combination disc springs with and without bearing surface using a 3,000 kN servo hydraulic test system. Fig. 3 shows the test device, and 16 pieces of disc springs that were composed of 2 pieces of a group in parallel and 8 groups in series were installed in the test device, each one had 200 mm outer diameter, 112 mm inner diameter, 16.2 mm height, 12 mm thickness and 4.2 mm solid height for disc spring-I without bearing surface, and 11.25 mm thickness and 4.95 mm solid height for disc spring-II with bearing surface, the material of disc springs was 50CrVA. The bearing forces of disc springs were

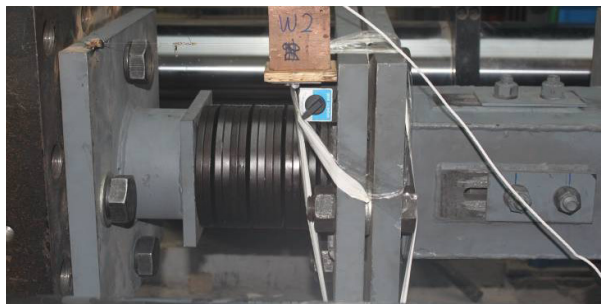


Fig. 3 Test setup of combination disc springs

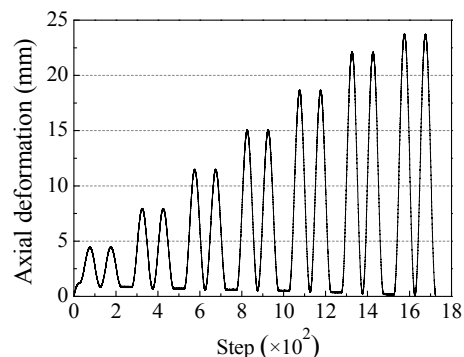


Fig. 4 Loading scheme of disc spring-I

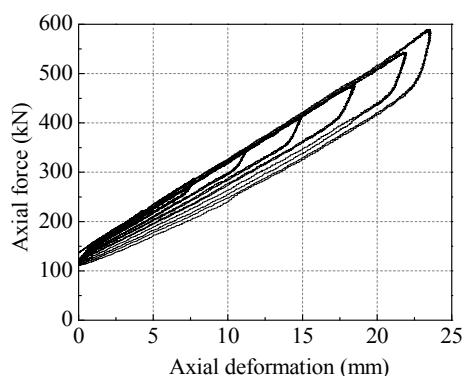


Fig. 5 Hysteretic responses of disc spring-I

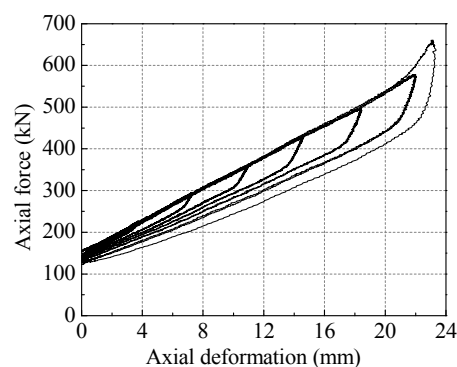


Fig. 6 Hysteretic responses of disc spring-I after fully compressed

measured by the load cell installed in the test machine, and the deformations were measured using a displacement meter installed on the test device.

Due to the cyclic compression loading scheme, as shown in Fig. 4, the hysteretic responses of disc spring-I are shown in Fig. 5, and after the disc spring-I was completely compressed, the hysteretic responses due to the cyclic compression loadings are shown in Fig. 6. It is observed that the disc spring-I has a certain ability of energy dissipation and also can recover to its initial state with no strength reduction or fracture when the unloading is complete, even after fully compressed. Because of the friction between disc springs and the inner tube, and the friction among disc springs, the bearing capacity and the energy dissipation capability increase with the increase of displacements.

Fig. 7 shows the cyclic compression loading scheme for disc spring-II, the hysteretic responses are shown in Fig. 8, and after the disc spring-II was completely compressed, the hysteretic responses due to the cyclic compression loadings are shown in Fig. 9. It is indicated that the disc spring-II has a certain ability of energy dissipation and also has a good self-centering capability, even after fully compressed.

Comparisons of the bearing and energy dissipation capacities for two kinds of disc springs before and after completely compressed are shown in Figs. 10-11, respectively. The bearing capacity and energy dissipation capacity of disc springs after completely compressed are improved,

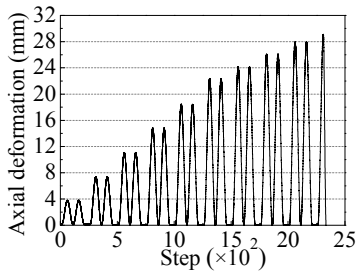


Fig. 7 Loading scheme of disc spring-II

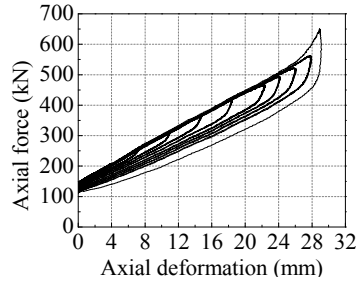


Fig. 8 Hysteretic curves of disc spring-II

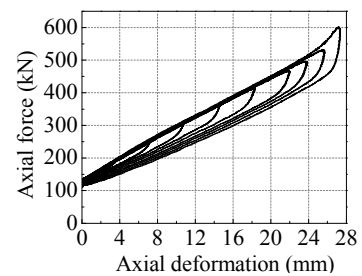


Fig. 9 Hysteretic responses of disc spring-II after fully compressed

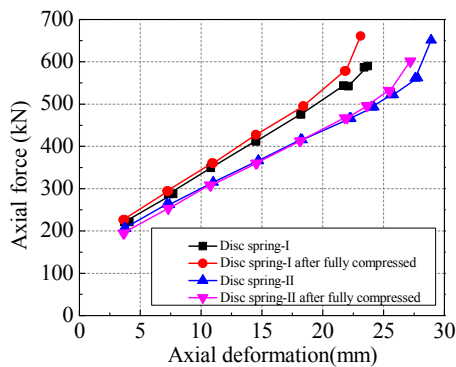


Fig. 10 Bearing capacity of disc springs

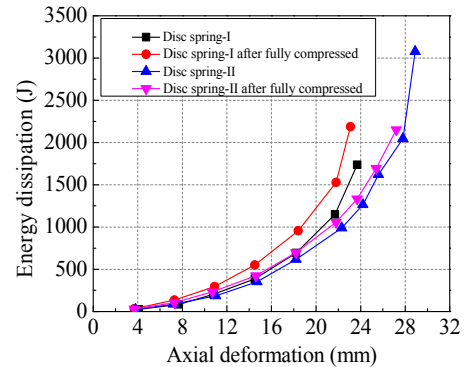


Fig. 11 Energy dissipation of disc springs

but the range of elastic deformation is reduced. The deformability of disc spring-II with bearing surface is better than that of disc spring-I without bearing surface, but the energy dissipation of disc spring-II is smaller than that of disc spring-I corresponding to the same deformation, and both the disc springs have similar ultimate bearing capacity and excellent self-centering behavior. For real application, the disc springs with or without the bearing surface can be selected according to the requirements for the deformability and stiffness.

3.2 Validation of FEDM

The FEDM was tested using a 3,000 kN servo hydraulic test system, as shown in Fig. 12, which consisted of a 215 mm × 215 mm × 6 mm box shaped cross section outer tube and a circular cross section inner tube with 54 mm outer diameter and 44 mm inner diameter and four non-asbestos-organic (NAO) materials with the dimension of 134 mm × 80 mm × 6 mm installed between the two tube members, the normal force was provided by the pre-stressed high strength bolts. The hysteretic responses of FEDM for different applied torque on the high strength bolts subjected to harmonic loading with amplitude of 20 mm and frequency of 0.02 Hz are shown in Fig. 13. The FEDM has stable energy dissipation ability, and which increases with the increase of normal force, and the measured friction forces of 75 kN, 100 kN, 125 kN, and 150 kN are respectively corresponding to the applied torques of 45 N·m, 60 N·m, 75 N·m, and 90 N·m, and which is about 1.69 times the applied torques.



Fig. 12 FEDM test system

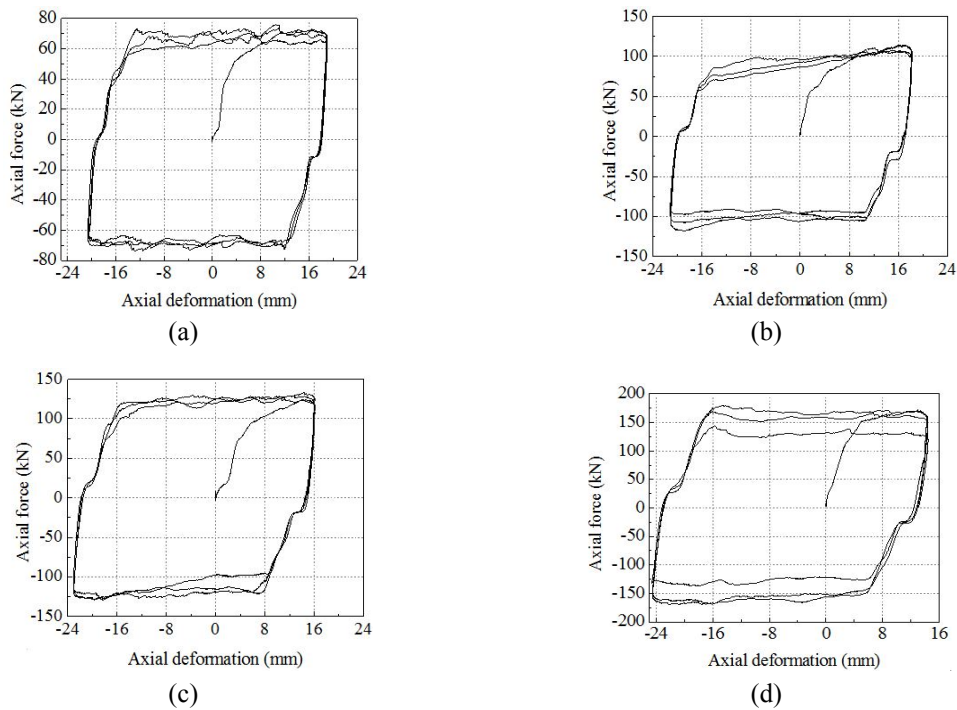


Fig. 13 Hysteretic responses of FEDM with friction force of (a) 75 kN; (b) 100 kN; (c) 125 kN; and (d) 150 kN

3.3 Behavior of a large-scale PS-SCED brace specimen

A large-scale PS-SCED brace specimen was fabricated and tested on a 3,000 kN servo hydraulic test system in the Structural Laboratory at Beijing University of Technology. As shown in Fig. 14, the PS-SCED brace specimen consisted of a 215 mm × 215 mm × 6 mm box shaped cross section outer tube and a circular cross section inner tube with 54mm outer diameter and 44 mm inner diameter, four steel plates with 10 mm thickness were welded to the inner tube to improve the bearing capacity and stability of the bracing system and several blocking plates were welded to the inner or outer tubes to enhance bearing force and push or pull the combination disc

springs, besides the outer tube was Q235 steel, the inner tube and blocking plates were Q345 steel, and the overall length of this specimen was 1680 mm and the length of inner tube was 1500 mm. Total 32 pieces of disc springs with 200 mm outer diameter, 112 mm inner diameter, 16.2 mm height and 12 mm thickness and 4.2 mm solid height were used to produce the expected restoring force for the bracing system and the pre-pressed force was set to 270 kN. Eight friction devices, which equipped with NAO friction pads with the dimension of 134 mm × 80 mm × 6 mm, were used to dissipate the input energy, and the initial friction forces were adjusted to 150 kN, 200 kN, and 300 kN, respectively, by changing the pre-tension force of high-strength bolts. The bearing forces of PS-SCED brace were measured by the load cell installed in the test machine, and the deformations of brace were measured using two displacement meters installed on the brace.

Fig. 15 shows the low cyclic reversed loading scheme, and the hysteretic responses of PS-SCED brace specimen with different friction forces are shown in Fig. 16. It is observed that the PS-SCED brace exhibits flag-shaped hysteretic responses with excellent self-centering capabilities, the energy dissipation ability is enhanced by increasing the friction forces of FEDMs, and almost no residual deformation occurs when the friction force is less than the pre-pressed force of combination disc springs, as shown in Figs. 16(b)-(c). However, the residual deformation of the brace specimen appears when the friction force is larger than the pre-pressed force of combination disc springs, as shown in Fig. 16(d), which is about 1.5 mm and only accounts for 12% of the maximum displacement of the brace in tension and compression. Therefore, the PS-SCED bracing system displays a stable and repeatable self-centering response with effective energy dissipation throughout the loading protocol, and it confirms that the proposed bracing system performs as predicted by the equations governing its mechanical behaviors.

Fig. 17 shows the skeleton curves of the PS-SCED brace with different friction forces under the low cyclic reversed loading, the stiffness of PS-SCED bracing system changes from the first



Fig. 14 Test system of PS-SCED brace

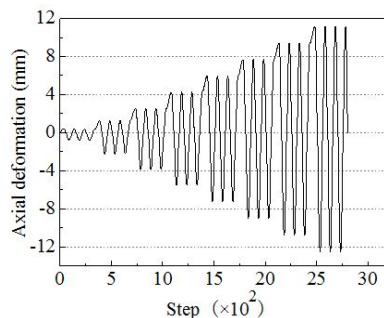


Fig. 15 Loading scheme of PS-SCED brace

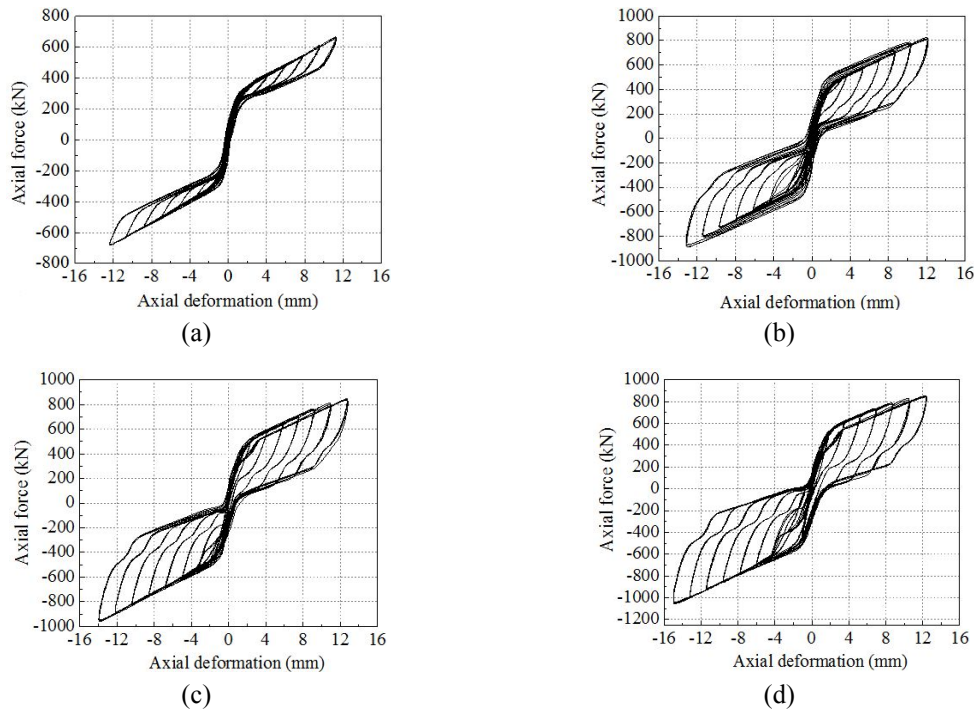


Fig. 16 Hysteretic responses of PS-SCED brace with friction force of (a) 0 kN; (b) 150 kN; (c) 200 kN; and (d) 300 kN

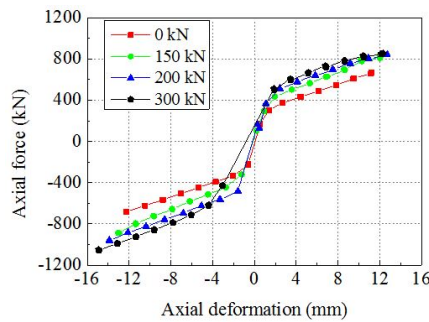


Fig. 17 Skeleton curves of PS-SCED brace with different friction forces

stiffness controlled by the inner and outer tube members to the second stiffness controlled by combination disc springs when the relative motion occurs between the two tube members, and the whole PS-SCED brace is in elastic state throughout the loading protocol.

To study the ultimate bearing capacity and ductility properties of the proposed PS-SCED brace, the ultimate bearing force experiments of the PS-SCED brace with the pre-pressed of 270 kN and the friction force of 240 kN provided by the FEDMs under the low cyclic reversed loading were conducted, Fig. 18 shows the buckling of connecting plates of the brace specimen in compression, and the hysteretic responses and the skeleton curve are shown in Figs. 19-20, respectively. The PS-SCED brace in tension exhibits a full flag-shaped hysteretic response with effective energy

dissipation and eliminates the residual deformation before the loading displacement reaches 12 mm, and the residual deformation occurs and increases with the increase of deformation of brace when the loading displacement increases from 12 mm to 28 mm, which is 9.2 mm and accounts for 32.9% of the maximum target tensile deformation. The PS-SCED brace in compression also exhibits a full flag-shaped hysteretic response and eliminates the residual deformation before the loading displacement reaches 24 mm which is the solid height of combination disc springs, with the increase of loading displacement, the controlled stiffness of PS-SCED brace changes from combination disc springs to the two tube members, thus the second stiffness increases suddenly, and the residual deformation appears and starts to increase, which is about 23.2% of the maximum target compressive deformation. In addition, the PS-SCED bracing system still can reduce the influence of residual deformations and dissipate energy effectively even the inner and outer tubes are already in the elastic-plastic stage.

The ultimate bearing forces of PS-SCED brace specimen are -1770 kN in compression and 1080 kN in tension, which have exceeded the design capacity of 954 kN, respectively, and the compressive ability is better than the tensile ability because the loads can be distributed to each part of the inner and outer tube members by the bracing system, and the ductility behavior in tension is better than that of the brace in compression. As a result, the ultimate compressive bearing capacity of the PS-SCED bracing system is determined by the bearing capacity of the two tube members and the compressive force of combination disc springs to reach the target deformation, and the strength and stability of the connecting plates should be satisfied the requirements of the ultimate bearing capacity.



Fig. 18 Buckling of connecting plates of PS-SCED brace

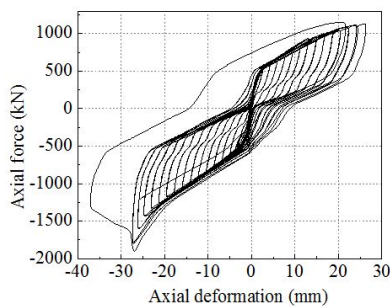


Fig. 19 Hysteretic responses of PS-SCED brace

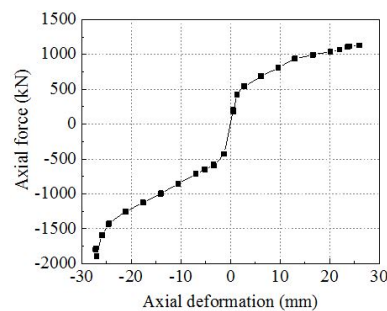


Fig. 20 Skeleton curve of PS-SCED brace

4. Comparison of prediction and test results

To verify the accuracy of the predictive equations governing the response of the PS-SCED bracing system, comparative analysis of prediction and test results for hysteretic responses of the PS-SCED brace specimen with the initial pre-pressed force of 270 kN and friction force of 0 kN, 150 kN, 200 kN, and 300 kN due to the low cyclic reversed loading are carried out, and the error is defined as Eq. (10) to further quantify the accuracy of the prediction.

$$J_{error} = \frac{\max |F_{pre} - F_{test}|}{\max |F_{test}|} \% \quad (10)$$

where F_{pre} and F_{test} are the bearing force of the bracing system corresponding to the loading scheme during the prediction and experiments, respectively.

Fig. 21 shows the comparison between the predicted and tested hysteretic responses of the PS-SCED bracing system, and the maximum bearing forces of the system corresponding to the loading displacement and the errors between the predicted force and the tested force are listed in Table 1. It is indicated that the predictive equations can accurately portray the mechanical behaviors of the PS-SCED bracing system, and the maximum error between the prediction and experiments is about 8.45%, 6.65%, 5.02%, 4.47% corresponding to the friction of 0 kN, 150 kN, 200 kN, and 300 kN, respectively.

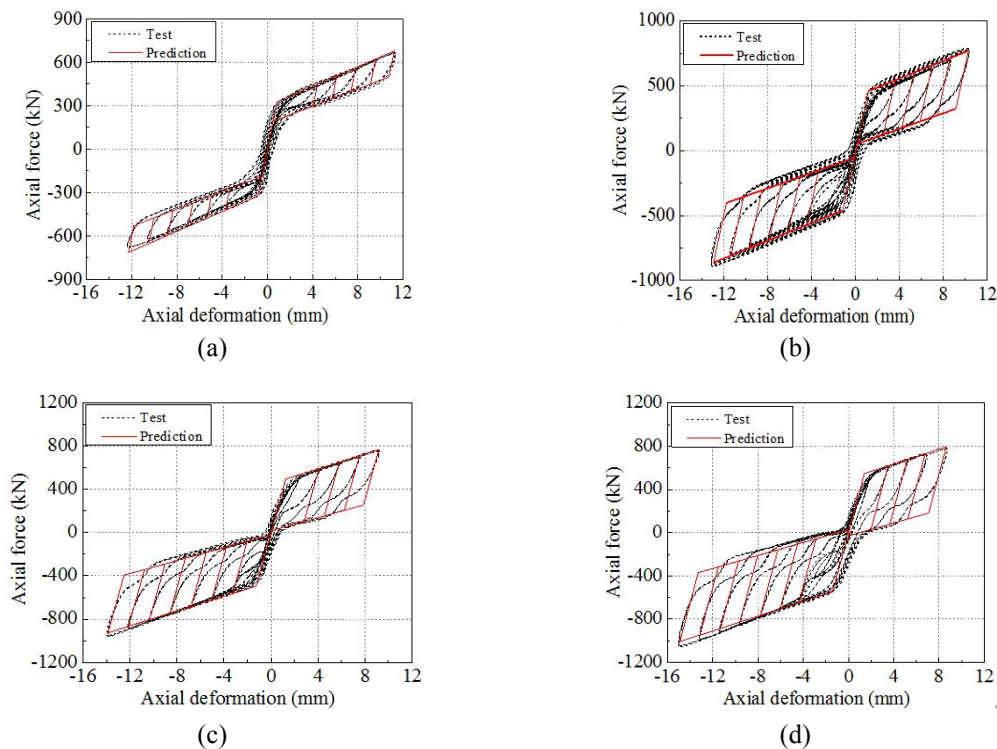


Fig. 21 Comparison of the predicted and tested hysteretic responses of PS-SCED brace with friction force of (a) 0 kN; (b) 150 kN; (c) 200 kN; and (d) 300 kN

Table 1 Maximum bearing force and errors of PS-SCED brace between prediction and experiments

Friction force = 0 kN												
Disp. (mm)	-12.3	-10.5	-8.8	-7.1	-5.3	-3.7	2.5	4.4	6.2	7.8	9.6	11.2
$\max F_{\text{test}}$ (kN)	-679.9	-623.4	-565.1	-504.4	-445.8	-389.2	319.1	433.1	487.8	543.8	612.9	667.4
$\max F_{\text{pre}}$ (kN)	-714.5	-653.0	-595.8	-535.1	-477.9	-422.1	331.1	447.3	505.4	561.8	621.7	678.2
J_{error} (%)	5.09	4.75	5.44	6.07	7.19	8.45	3.8	3.31	3.61	3.30	1.42	1.61
Friction force = 150 kN												
Disp. (mm)	-12.9	-11.4	-9.7	-7.9	-6.2	-4.5	3.6	5.3	7.0	8.6	10.3	12.1
$\max F_{\text{test}}$ (kN)	-888.6	-794.7	-722.8	-659.6	-582.5	-513.7	503.1	568.0	629.4	701.2	776.8	809.2
$\max F_{\text{pre}}$ (kN)	-837.1	-783.3	-725.9	-664.5	-606.1	-547.8	518.6	576.9	634.1	688.6	746.4	805.6
J_{error} (%)	5.80	1.43	0.42	0.75	4.05	6.65	3.09	1.56	0.75	1.80	3.92	0.45
Friction force = 200 kN												
Disp. (mm)	-13.89	-12.1	-10.4	-8.6	-6.8	-5.1	4.1	5.8	7.5	9.2	11.0	12.7
$\max F_{\text{test}}$ (kN)	-955.1	-883.8	-825.2	-755.1	-691.7	-626.2	576.7	644.8	696.8	752.7	798.2	845.2
$\max F_{\text{pre}}$ (kN)	-907.2	-847.5	-787.5	-727.4	-666.2	-606.5	573.1	632.4	691.1	747.2	807.8	867.2
J_{error} (%)	5.02	4.12	4.63	3.66	3.69	3.15	0.62	1.91	0.82	0.73	1.21	2.60
Friction force = 300kN												
Disp. (mm)	-14.9	-13.2	-11.3	-9.6	-7.8	-6.1	-4.4	3.5	5.2	6.8	8.6	—
$\max F_{\text{test}}$ (kN)	-1048.6	-987.3	-921.4	-853.4	-786.4	-715.1	-620.9	595.7	669.1	733.5	778.3	—
$\max F_{\text{pre}}$ (kN)	-1006.9	-946.3	-884.4	-826.2	-764.54	-704.8	-648.6	617.5	675.2	730.1	793.2	—
J_{error} (%)	3.98	4.16	4.02	3.19	2.78	1.45	4.47	3.66	0.91	0.48	1.91	—

5. Conclusions

A new type of PS-SCED bracing system that combines friction energy dissipation mechanisms between the inner and outer tube members with the pre-pressed disc springs self-centering mechanism was developed and experimental studied in this contribution. The mechanics and the equations governing the design and hysteretic responses of the bracing system were presented. A series of validation tests of components comprising the self-centering mechanism of combination disc springs, the friction energy dissipation mechanism, and a large scale PS-SCED brace specimen were carried out due to the low cyclic reversed loadings. Test results indicated that the combination disc springs had a certain ability of energy dissipation and excellent self-centering behavior, even after fully compressed, and the friction energy dissipation device exhibited ideal elastic-plastic performance with full hysteretic responses. Experiments of a large scale PS-SCED bracing system demonstrated that the bracing system performed as predicted by the equations governing its mechanical behaviors, which exhibited a stable and repeatable flag-shaped hysteretic response with excellent self-centering capability and effective energy dissipation throughout the loading protocol, almost no residual deformation occurred when the friction force was less than the pre-pressed force of disc springs. However, the residual deformation of the brace occurred when the friction force was larger than the pre-pressed force of disc springs, which was approximately 12% of the maximum the brace deformation, and it could be controlled by adjusting the ratio of initial pre-pressed force of disc springs to the friction force of friction energy

dissipation devices. The ultimate bearing capacity experiments indicated that the compressive ability was better than the tensile ability and the ductility behavior in tension was better than that of the brace in compression, and the ultimate compressive bearing capacity of the PS-SCED bracing system was determined by the bearing capacity of the two tube members and the compressive force of disc springs to reach the target deformation. For real application, the strength and stability of the connecting plates should be designed to satisfy the requirements of the ultimate bearing capacity.

Acknowledgments

The writers gratefully acknowledge the partial support of this research by the National Natural Science Foundation of China under Grant No. 51322806 and No. 51578058, the Fundamental Research Funds for the Central Universities under Grant No. 2014JBZ011, and the National Basic Research Program of China (973 Program) under Grant No. 2011CB013606 and 2011CB013603.

References

- Cao, Z.L., Guo, T., Xu, Z.K. and Lu, S. (2015), "Theoretical analysis of self-centering concrete piers with external dissipators", *Earthq. Struct.*, **9**(6), 1313-1336.
- Christopoulos, C., Tremblay, R., Kim, H.J. and Lacerte, M. (2008), "Self-centering energy dissipative bracing system for the seismic resistance of structures: Development and validation", *J. Struct. Eng. ASCE*, **134**(1), 96-107.
- Erochko, J. and Christopoulos, C. (2014), "Seismic response of six-story steel frame building with self-centering energy-dissipative (SCED) braces combined with linear viscous dampers", *Proceedings of the 10th U.S. National Conference on Earthquake Engineering, Frontier of Earthquake Engineering*, Anchorage, Alaska, July.
- Garlock, M., Ricles, J. and Sause, R. (2005), "Experimental studies of full-scale posttensioned steel connections", *J. Struct. Eng. ASCE*, **131**(3), 438-448.
- Garlock, M., Sause, R. and Ricles, J. (2007), "Behavior and design of posttensioned steel frame systems", *J. Struct. Eng. ASCE*, **133**(3), 389-399.
- Kim, H.J. and Christopoulos, C. (2009), "Seismic design procedure and seismic response of post-tensioned self-centering steel frames", *Earthq. Eng. Struct. Dynam.*, **38**(3), 355-376.
- Marino, E.M. and Nakashima, M. (2006), "Seismic performance and new design procedure for chevron-braced frames", *Earthq. Eng. Struct. Dynam.*, **35**(4), 433-452.
- Miller, D.J. (2011), "Development and experimental validation of self-centering buckling-restrained braces with shape memory alloy", Ph.D. Dissertation; University of Illinois at Urbana-Champaign, Champaign, IL, USA.
- Miller, D.J., Fahnestock, L.A. and Eatherton, M.R. (2011), "Self-centering buckling-restrained braces for advanced seismic performance", *Structures Congress*, NV, USA, April.
- Miller, D.J., Fahnestock, L.A. and Eatherton, M.R. (2012), "Development and experimental validation of a nickel-titanium shape memory alloy self-centering buckling-restrained brace", *Eng. Struct.*, **40**, 288-298.
- Morgen, B.G. and Kurama, Y.C. (2007), "Seismic design of friction-damped precast concrete frame structures", *J. Struct. Eng. ASCE*, **133**(11), 1501-1511.
- Morgen, B.G. and Kurama, Y.C. (2008), "Seismic response evaluation of posttensioned precast concrete frames with friction dampers", *J. Struct. Eng. ASCE*, **134**(1), 132-145.
- Sabelli, R., Mahin, S.A. and Chang, C. (2003), "Seismic demands on steel-braced frame buildings with buckling-restrained braces", *Eng. Struct.*, **25**(5), 655-666.
- Tremblay, R., Lacerte, M. and Christopoulos, C. (2008), "Seismic response of multistory buildings with

- self-centering energy dissipative steel braces”, *J. Struct. Eng. ASCE*, **134**(1), 108-120.
- Uang, C.M., Nakashima, M. and Tsai, K.C. (2004), “Research and application of buckling-restrained braced frames”, *Int. J. Steel. Struct.*, **4**(4), 301-313.
- Xu, L.H., Li, Z.X. and Lv, Y. (2014), “Nonlinear seismic damage control of steel frame-steel plate shear wall structures using MR dampers”, *Earthq. Struct.*, **7**(6),937-953.
- Zhou, Z., He X.T., Wu, J., Wang, C.L. and Meng, S.P. (2014), “Development of a novel self-centering buckling-restrained brace with BFRP composite tendon”, *Steel Compos. Struct., Int. J.*, **16**(5), 491-506.
- Zhu, S.Y. and Zhang, Y.F. (2007), “Seismic behavior of self-centering braced frame buildings with reusable hysteretic damping brace”, *Earthq. Eng. Struct. Dyn.*, **36**(10), 1329-1346.
- Zhu, S.Y. and Zhang, Y.F. (2008), “Seismic analysis of concentrically braced frame systems with self-centering friction damping braces”, *J. Struct. Eng. ASCE*, **134**(1), 121-131.

CC